Chapter

Failure Modes in Fiber Reinforced Composites and Fracture Toughness Testing of FRP

Evren Meltem Toygar and Ahmet Gulakman

Abstract

In this paper, interlaminar fracture behavior of woven-fabric-reinforced glass/epoxy composites has been investigated experimentally and numerically. The mechanical properties of this composite were studied and Mode I (Tensile Opening) DCB (Double Cantilever Beam) tests were performed on Fiber Reinforced Composite (FRP) specimens to determine the delaminating resistance of composite laminates used for structural applications. Techniques for measuring the interlaminar fracture toughness, K_{IC} data of woven-fabric-reinforced glass/epoxy composite materials, are highlighted under the consideration of ASTM Standard D5528–01 and test methods ISO 15024, DIN EN ISO 75-1 and DIN EN ISO 75-3. The obtained test results were apparently consistent with the assumptions of the CCM (Compliance Calibration Method) that was used to obtain the interlaminar critical SERR (strain energy release rate), G_{IC}. Finite element analysis was conducted to validate the closed form solution. The use of obtained mechanical properties data in finite element analyses utilizing fracture mechanics are examined. Results show a good agreement between experimental and numerical solutions.

Keywords: interlaminar fracture toughness, fracture mechanics, woven-fabric-reinforced glass/epoxy composites, DCB test method, finite element method

1. Introduction

Woven fabric reinforced composites are the most important and widely used forms among textile structural composites. In recent years, fracture mechanics has found an extensive applications in damage analysis of composite laminates, especially in delamination analysis. Delaminations may occur during manufacture because of incomplete curing or may result from impact damage; or they may result from the interlaminar stresses that develop at stress-free edges or discontinuities. It has been mentioned that delamination in a composite laminate usually occurs at the interface of different oriented plies and tends to grow and also it can be a major problem for laminated composite structures. Sometimes, delaminations may also be result of contamination of the pre-preg, the poor ply adhesion, or they may form locally in regions of high void content. The problems of interlaminar performance

are discussed along with the technique used to measure them and the fracture mechanics principles applied to improve them, because laminated composite materials have been increasingly used in large transport aircraft structures due to their low density compared to other materials. The delamination resistance of laminated composites can be measured by critical SERR (strain energy release rates). The DCB (Double Cantilever Beam) is the most popular specimen configurations in the experimental determination of Mode I interlaminar fracture toughness. Aliyu and Daniel [1], used conventional double cantilever beam specimens with different configurations to measure the Mode I fracture toughness in a graphite/epoxy composite. The effect of stacking sequence on energy release rate distribution across the specimen width the multidirectional DCB specimens are determined by Davidson et al. [2]. They investigated eight different stacking sequences, with the delamination growth between 30°/−30° interface.

Sun and Zheng [3], analyzed the distribution of strain energy release rate, G at the crack fronts of double cantilever beam specimens by means of the plate finite element. They found a boundary layer phenomenon in the distribution of G at the crack front, which causes the strain energy release rate to vary along the straight crack front. Toygar et al. [4] measured the fracture toughness value of carbon/epoxy composite materials by using the CMOD (crack mouth opening displacement) method experimentally using SENT (Single Edge Notch Tension) specimens. The finite element study was carried out by using 2-D model to obtain the fracture toughness value of woven carbon/epoxy composite numerically with the ABAQUS finite element software package. Mode I DCB tests were performed on carbon/epoxy woven laminates in weave style, which means as plain weave such as $[0°/90°]_{16}$, where 16 means the number of layers, lay-up specimens by Morais et al. [5]. The starter crack was created at mid-thickness, between the 0° and 90°, stand for the directions of fill and warp strips, respectively. The test results were apparently consistent with the assumptions of the CBT (Corrected Beam Theory) that was used to obtain the interlaminar critical SERR, G_{IC}. The measured values were higher than those of unidirectional $[0°]_{24}$ specimens, especially the final propagation values. A finite-element analysis confirmed the applicability of the CBT for interlaminar propagation along the two [0°/90°] interfaces. They have found that the intralaminar G_{IC} is significantly smaller than the interlaminar G_{IC}. This will prevent pure interlaminar propagation in multi-directional specimens with high interlaminar fracture toughness. The interlaminar fracture is a common mode of failure for composite materials, especially in laminated architectures [6–8]. Interlaminar fracture mechanics has proven useful for characterizing the onset and growth of delaminations. Delamination onset and debonding in fracture toughness specimens (such as Double Cantilever Beam Specimen) and laboratory size coupon type specimens (such as the skin/stringer debond specimen) has been investigated [9–11].

In this study, the influence of test parameters on Mode I delamination resistance is examined. A detailed discussion on test method and data reduction schemes for Mode I interlaminar fracture toughness characterization of composite laminates have been done by considering the test parameters such as width, different fiber orientation and lay-up and ext. In the case of laminated composites, the Griffith criterion is applied to calculate the critical amount of energy required to propagate a crack and DCB test is used to obtain this material property. In a result of this, DCB tests on woven-fabric-reinforced glass/epoxy specimens were performed in accordance with ASTM Standard D5528–01 and ISO 15024, DIN EN ISO 75-1 and DIN EN ISO 75-3 Standards [12–16] to measure the delamination resistance under Mode I loading. Therefore, the present research has been focused on the characterization of delamination growth in laminated structures and has been done to determine Mode I interlaminar fracture toughness, K_{IC} of woven laminates $[0°/90°]_{16}$ and $[\pm 45°]_{16}$ lay-up

composites such as in weave style as plain weave and with 16 number of layers. The obtained experimental data were reduced by using data reduction technique CCM (Compliance calibration method) to determine the critical SERR, G_{IC}. CCM generates a least squares plot of log ($\delta i/Pi$) versus log (ai), where i represents the number of specimen and changes from 1 to minimum 5 and P and δ represent the measured values of load and load point displacement, respectively during the test, and a represents the crack length, to use the visually observed delamination onset values and all the propagation values [17]. Additionally, fracture mechanics based finite element models of described DCB tests were developed to confirm the experimental results. The finite element analysis has been carried out to accomplish the delamination analysis of the specimen. Critical load levels, the geometrical and material properties of the test specimens were used as input data for the analysis to evaluate the Mode I energy release rate at the onset of delamination crack propagation.

2. Materials, sample preparation and measurement of mechanical properties

Delamination growth has typically been related to the cyclic SERR, G, for composite materials, using a power law expression [18–20], known as the Paris Law. Fracture toughness may be described as the critical energy that a material may absorb before failure. Independent of specimen geometry, this property describes the general resistance of a material to delaminate [21].

In this study, DCB specimens having density 1,72 g/cm^3 were manufactured in Dokuz Eylul University laboratory from the woven-fabric-reinforced glass/epoxy materials and the detail of sample cutting $[0°/90°]_{16}$ and $[\pm 45°]_{16}$ woven DCB specimens are given in **Figure 1a** and **b**, respectively. All were prepared from manufactured woven composite plate. The prepared composite plate has sixteen laminas and has a volume fraction of glass fiber of approximately 60%. During manufacturing, a thin non-adhesive Teflon film with 0.07 mm thickness were placed at the midplane (between 8th and 9th plies) at one end to simulate an initial delamination by considering ASTM Standard D5528–01 and British test method ISO 15024.

The mechanical tests to obtain the mechanical properties were carried out by using the prepared specimen which is given in **Figure 2**. The universal mechanical test machine, which is used, is available with different clamping techniques and accessories such as digital click-on extensometer from Zwick Roell. The width and thickness of each specimen were measured using a micrometer, at the center and each end. The tensile test was conducted following ASTM Standard E-681 [22].

2.1 Video extensometer

Video extensometer ME-46 is a high resolution and non-contact strain measurement system which is capable of measuring both longitudinal and lateral strain, modulus and Poisson ratio of polymer composites (see in **Figure 3a**). The advantage of the non-contacting method is that the strain is directly measured and end-effects from the gripping system need not to be considered [24] and for non-contact strain measurement the detail is given in **Figure 3b**. The measurement was carried out optically and there is no requirement for physical contact between the extensometer and the test specimen. Therefore, it can be applied to all sample without and slippage and related test specimen breakage problems [23]. The mechanical properties of this woven-fabric-reinforced glass/epoxy composite were obtained experimentally by using video extensometer under the consideration of ASTM Standards and were given in **Table 1**.

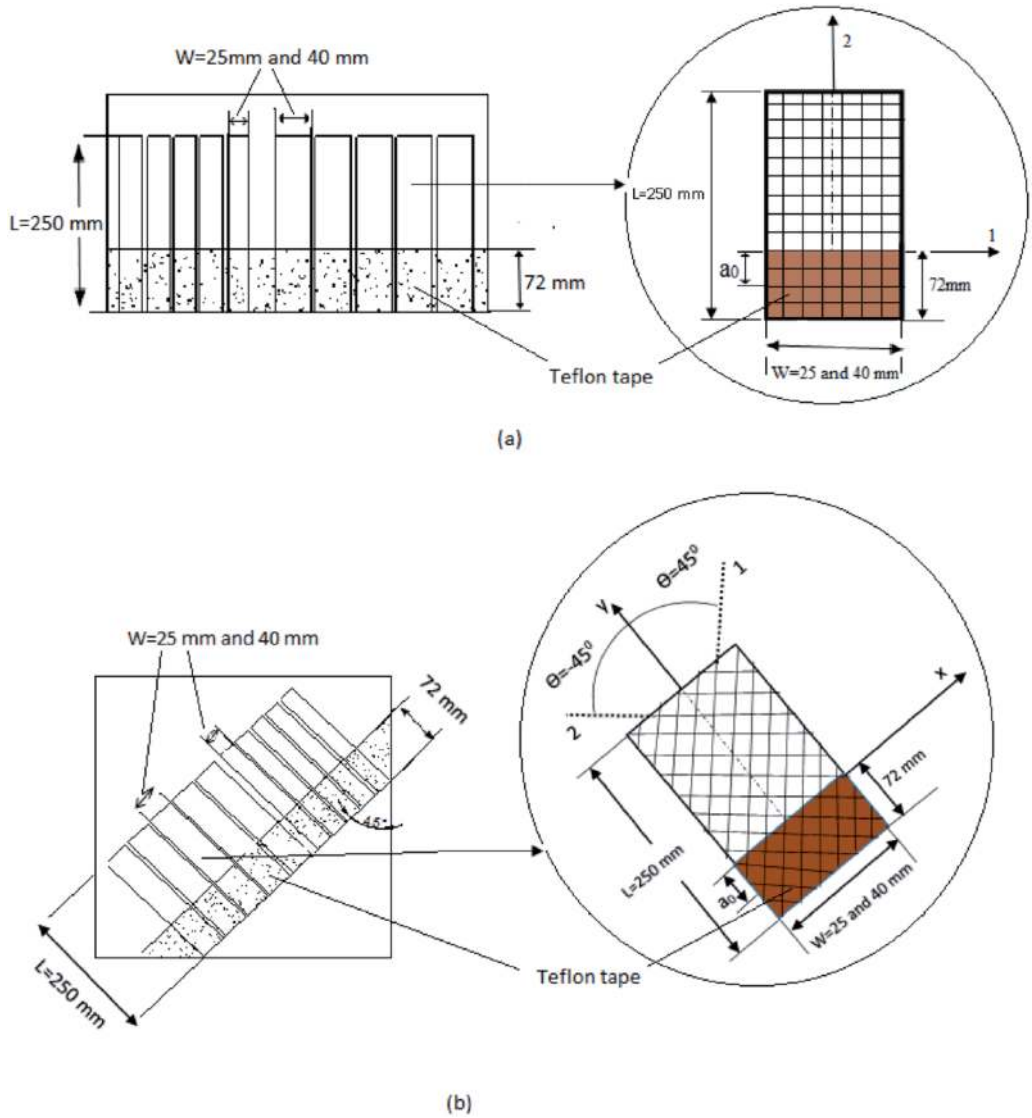

Figure 1.
The detail of cutting of sample from manufactured woven-fabric-reinforced glass/epoxy composite plate a) (0°/90°) fiber orientation, b) (±45°) fiber orientation.

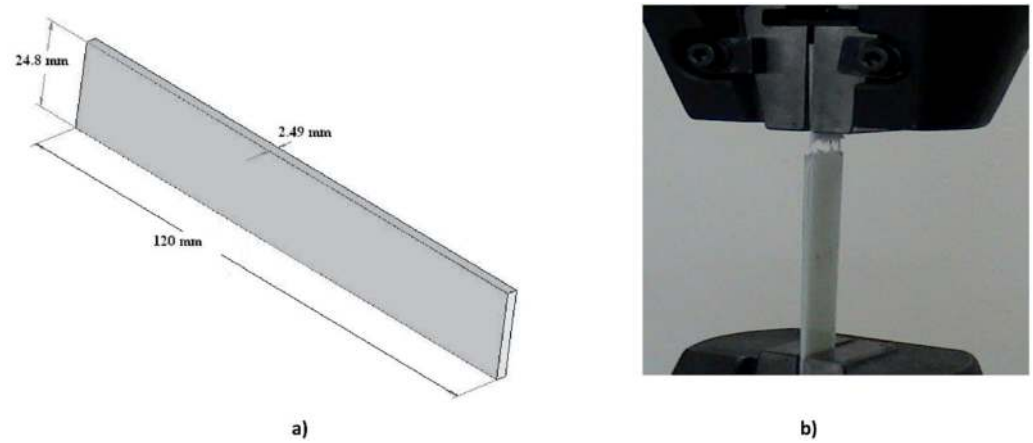

Figure 2.
a) Geometries of test specimen for mechanical properties testing, b) view of tension test.

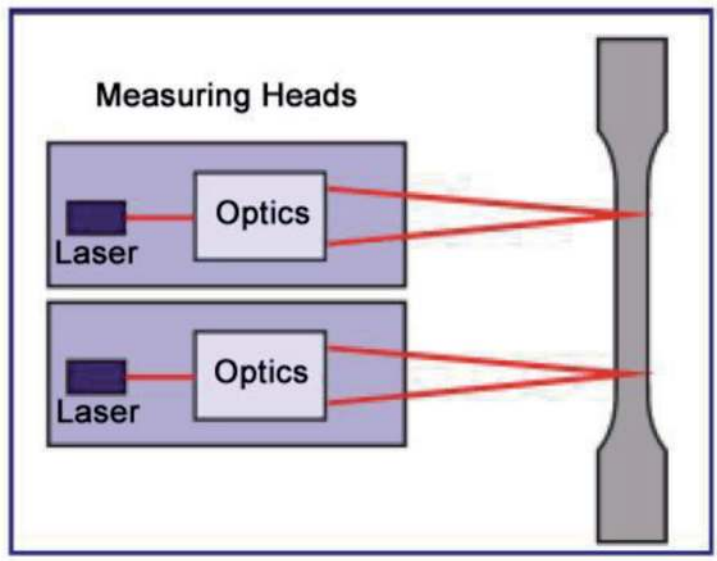

(a)

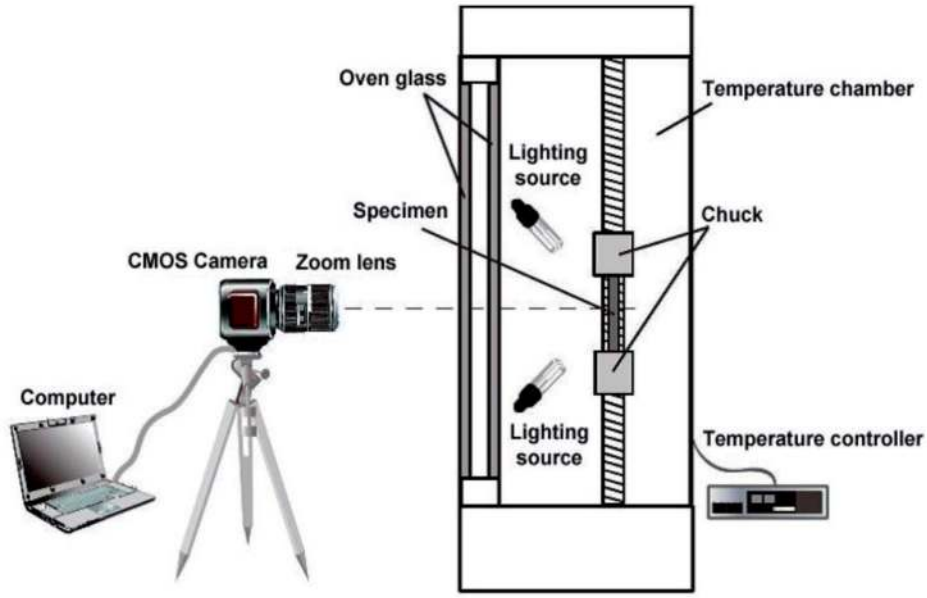

(b)

Figure 3.
a) Schematic detail of video extensometer [23], b) schematic drawing of the non-contact varying temperature deformation measuring system [24].

2.2 Optical deformation and strain measurement system

Aramis [21] is an optical technique from GOM (Gesellschaft fur Opticsche Mestechnik), Germany. It can be used to non-destructively measure the deformation and strain profiles of an object surface under loading. It has advantages of simple specimen preparation, large measuring area, non-contact and full field measurement, no laser illumination, material independent determination, full field and graphical results, three-dimensional results and good mobility. Its capabilities

Materials	Density (g/cm^3)	Poisson ratio (ν)		Modulus of elastisity (E) (Gpa)		Shear modulus (G) (Gpa)
		ν_{12}	ν_{21}	E_1	E_2	G_{12}
$(0°/90°)_{16}$	1.72	0.28	0.28	28.2	28.2	4.7

Table 1.
Physical and mechanical properties of woven specimen in the principal material direction.

include materials testing, stability estimating, components dimensioning, nonlinear behavior examination, creep and aging processes characterization. Because the deformation and strain of an object under mechanical loading is associated with its structure integrity, the abnormalities and irregularities in deformation and strain profiles indicate the damage presence. It can be adapted to assess the structural integrity and non-destructive testing of polymer composites.

2.3 DCB specimen for interlaminar fracture toughness

The average specimen width, b, was 25 mm and/or 40 mm for DCB specimen and an illustration of it was given in **Figure 4**. The hinges were mounted on the top and bottom surfaces of the end of DCB specimen arms by using an epoxy adhesive, which was cured. The average thickness h, was 2.5 mm, the initial delamination length a_0, was produced by using Teflon has a distance 47 mm from the line of load application to the crack tip. The DCB specimens were tested in a tensile testing machine where a tensile load was applied to the specimens through hinges (see **Figure 5**). Immediately before testing, a thin layer of black paint and marked in 1 mm increments were mounted on the specimen to observe crack propagation, starting from the tip of the insert to a length of 47 mm as shown in **Figure 6**. Tests were carried out in a AG-50kNG Shimadzu universal testing machine at 2 mm/min crosshead speed. Following the procedures of ISO 15024:2001, a pre-cracking cycle was performed and given in **Figures 7–10** for different orientation and width of specimen. Initiation values from the insert were then recorded. Further measurements were made in an additional loading cycle, where the crack was allowed to propagate. During the DCB tests, load, displacement, and temperature

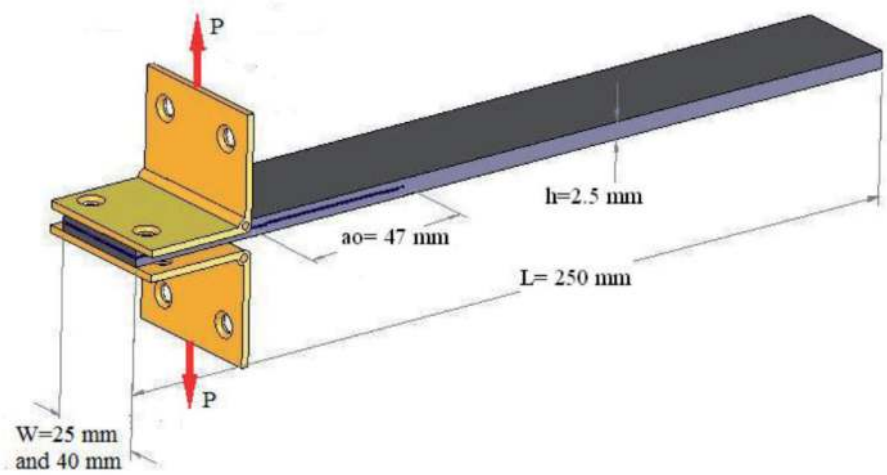

Figure 4.
The dimensions of DCB test specimen.

Figure 5.
Experimental setup for DCB specimen and fracture in DCB test.

Figure 6.
Overview of loading device and test setup of DCB specimen and delamination a) initially b) progress.

measurements were recorded and video images of the delamination growth were also recorded.

The specimen was subjected to displacement controlled loading and usually experiences stable delamination growth allowing several values of interlaminar fracture toughness to be determined along the specimen's length. As the delamination grows, fiber bridging usually occurs increasing the energy required to propagate further delamination ISO 15025:2001. Interlaminar fracture mechanics was used for characterizing the onset and growth of delaminations and it's calculation is based on experimental CCM as described by ASTM D5528–01. The compliance method is an effective method for determining the fracture characteristics of brittle materials. Fracture toughness is related to the amount of energy required to create fracture surfaces. There are several ways in which initiation and propagation values of G_{IC} can be derived from the recorded load–displacement data. Initiation of delamination is determined by deviation from linearity. G_{IC} can be calculated using the load and displacement at the point of non-linearity of the load–displacement curve. The load–displacement data were then recorded. The unloading curve was also registered, as in case of significant permanent deformations and/or non-linearity. The camera was positioned at a distance 1000 mm away from the specimen surface. Images are captured during the test using two CCD-cameras to get CMOD.

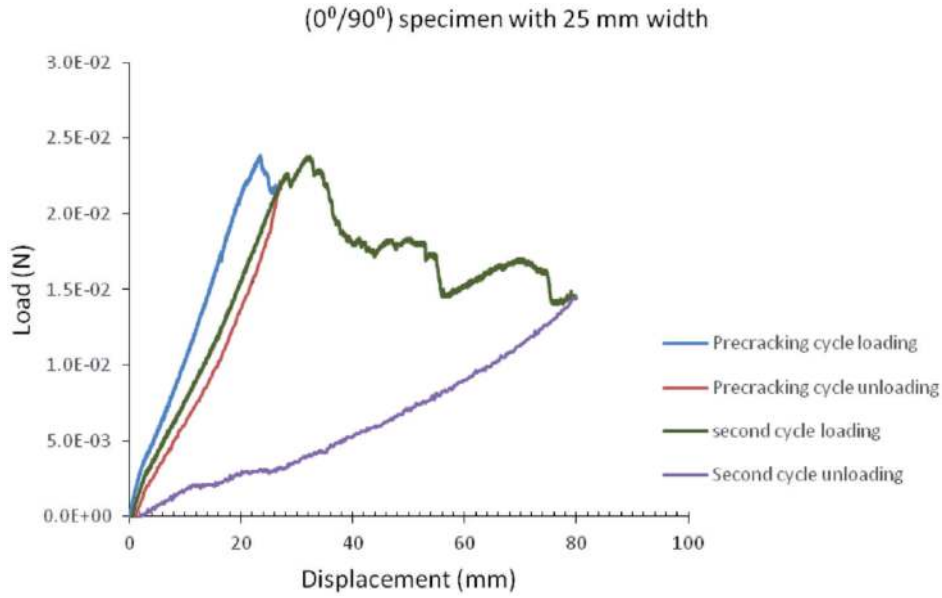

Figure 7.
Load–displacement characteristics for sample 4, woven $[0°/90°]_{16}$ with 25 mm width.

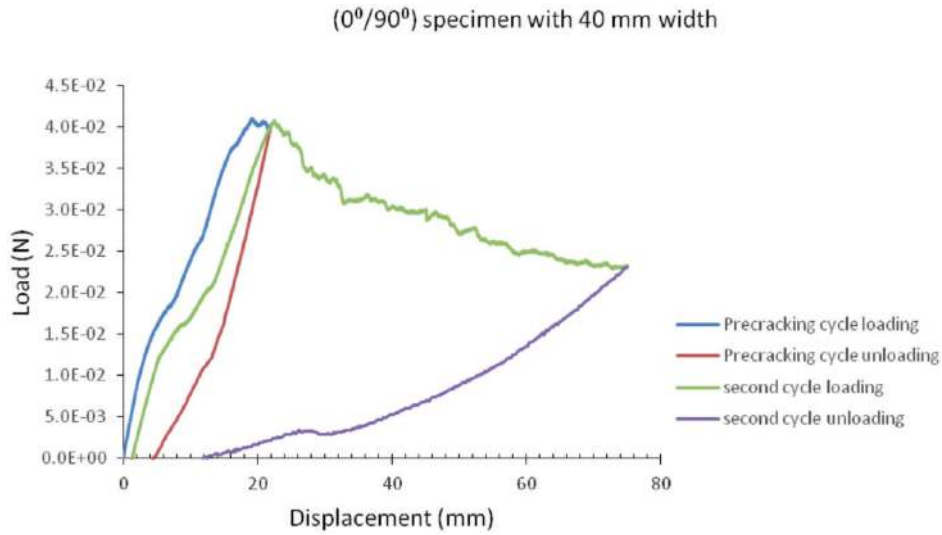

Figure 8.
Load–displacement characteristics for sample 4, woven $[0°/90°]_{16}$ with 40 mm width.

In DCB tests, there are four test groups including: *Type 1–1*, *Type 1–2*, *Type 2–1*, *Type 2–2* and they are given in **Table 2**. In *Type X-X* notation, first one denotes direction of woven and second one denotes the width of the DCB specimen. Therefore, *Type 1–1* represents the woven $[0°/90°]_{16}$ with 25 mm width specimen, *Type 1–2* represents the woven $[0°/90°]_{16}$ with 40 mm width specimen, *Type 2–1* represents the woven $[\pm 45°]_{16}$ with 25 mm width specimen, *Type 2–2* represents the woven $[\pm 45°]_{16}$ with 40 mm width specimen. The tests were performed at constant room conditions of 22°C and humidity ratio was 50% in respect of the conditions were needed for standards.

To observe the (delamination) crack growth and to identify crack extension Δa in mm during the loading, the gripped hinges were pulled apart with a crosshead speed of 2 mm/min in displacement control until satisfactory crack

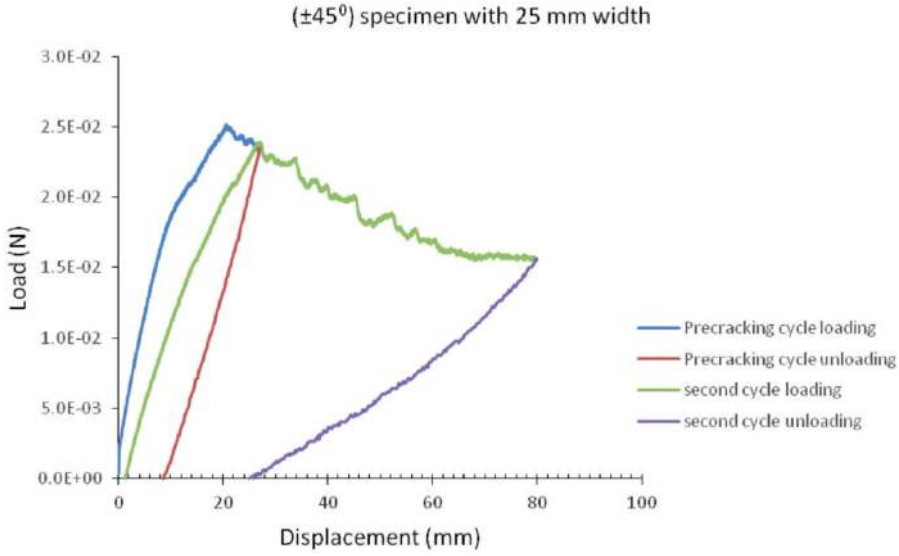

Figure 9.
Load–displacement characteristics for sample 3, woven $[\pm 45°]_{16}$ with 25 mm width.

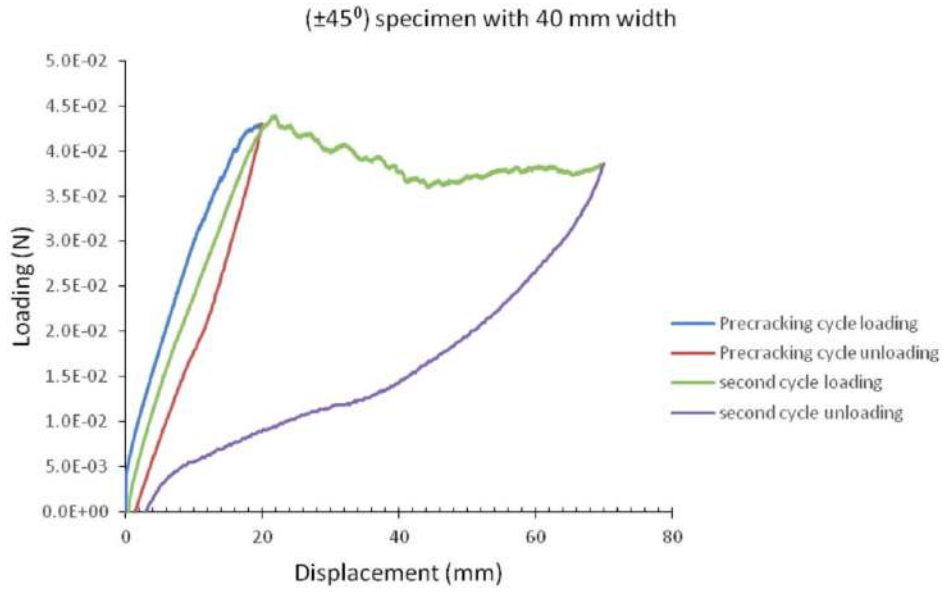

Figure 10.
Load–displacement characteristics for sample 4, woven $[\pm 45°]_{16}$ with 40 mm width.

growth was occurred in the specimen. During the test, the characteristic load–displacement curves were obtained for all test groups and the mean characteristic behavior for each group has been given in **Figures 7–10**. One issue with this test is the slope of the compliance changes as the crack propagates along the specimen. To get the value n, the ratio between the slope of the log c, which is the logarithm of compliance values that is obtained for the system, and log a is the logarithm of the crack length is obtained. Both testing and post processing were conducted similarly for each specimen. First the loading has been obtained with a cross-head speed of 2 mm/min in displacement control up to pre-cracking occurs. Then specimen was unloaded at a constant cross head rate of up to 25 mm/min, the position of the tip of the pre-crack on both edges of the specimen was marked and the procedure was repeated to extent the crack further. Subsequent

DCB specimen type	Fiber direction	Specimen width *b* (in mm)	Total number of *DCB* specimens used in experiment	Obtained average max load (*N*)	Obtained average G_{IC} (J/mm^2)
Type1–1	woven $[0°/90°]_{16}$	25	5	26.48	0.586
Type1–2	woven $[0°/90°]_{16}$	40	5	40.78	0.563
Type2–1	woven $[\pm 45°]_{16}$	25	5	23.18	0.544
Type2–2	woven $[\pm 45°]_{16}$	40	5	33.72	0.530

Table 2.
Fiber directions and width of DCB test specimens used in experiments and fracture energies in pure mode I obtained by DCB under consideration of ASTM standard D5528–01.

measurements were made in an additional loading cycle, where the delamination was allowed to propagate. The unloading curve was also registered, as in case of significant permanent deformations and/or non-linearity. Data reduction was performed according to CCM.

3. Data reduction to obtain interlaminar fracture toughness and energy release rate

There are many analysis methods available for analyzing DCB data. The compliance is defined as the opening displacement measured at the load application points divided by the applied load. Many of the compliance methods are based upon the expression (assuming a linear load-deflection relation): the interlaminar fracture can be calculated by compliance or compliance calibration method, which assumes linear elastic behavior such as [25].

$$G_{IC} = \frac{P_c^2}{2B}\frac{dc(a)}{da} \tag{1}$$

where; P_c is the critical load, a is crack length, B is the specimen width, and $c = \delta / P$ shows the compliance and δ is the CMOD. The compliance values were used to fit versus curve, leading to the critical energy release rate G_{IC}, which is determined by three methods: MBT (Modified Beam Theory), CCM, MCCM (modified compliance calibration method) differed by not more than 3.1%, none of the them were superior to the others [26]. Therefore, G_{IC} for linear elastic material behavior CCM as;

$$G_{IC} = \frac{nP_c\delta}{2Ba} \tag{2}$$

where; P_c is the critical load, a is crack length, B is the specimen width, δ is load point displacement in mm. n is the ratio between the slope of the $\log \delta_i / P_i$, which is the compliance of the system and the index i represents the total number of samples and changes from 1 to 5, and P and δ represent simultaneously measured values of load

and displacement, respectively during the test, and log a where a represents the crack length. Using a least squares approximation, the slope of log c versus log a yields the value of n for different types of specimen. The mean compliance calibration graphs for different test groups are obtained and given in **Figures 11–14**. According to Castiglione's principle using the relation between the displacement and strain energy (U) as follows:

$$c = \frac{1}{P}\frac{dU}{dP} \tag{3}$$

The CCM was applied to measure the crack growth in each test. Mode I interlaminar fracture toughness values were calculated by means of the following fracture toughness equation:

$$K_{IC} = \sqrt{EG_{IC}} \tag{4}$$

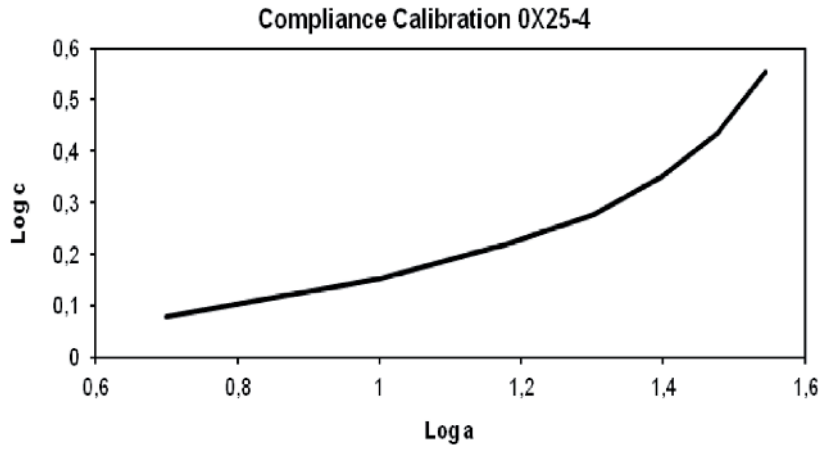

Figure 11.
Curve for slope of log c vs. log a, 'n' for sample 4 woven $[0°/90°]_{16}$ with 25 mm width.

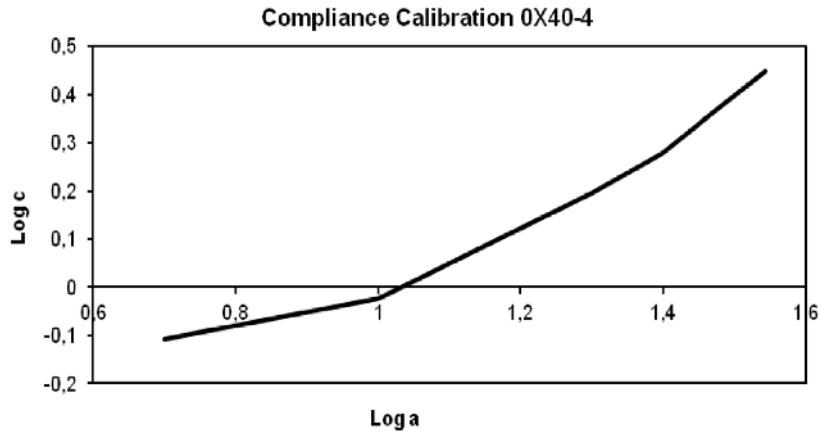

Figure 12.
Curve for slope of log c vs. log a, 'n' for sample 4 woven $[0°/90°]_{16}$ with 40 mm width.

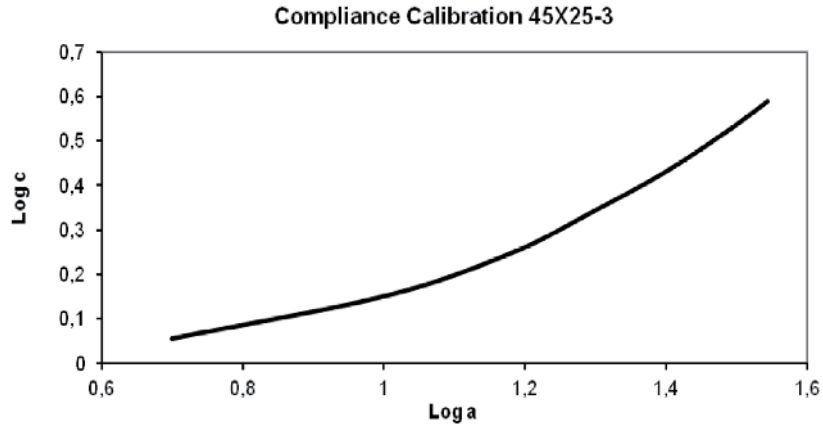

Figure 13.
Curve for slope of log c vs. log a, 'n' for sample 3 woven $[\pm 45^\circ]_{16}$ with 25 mm width.

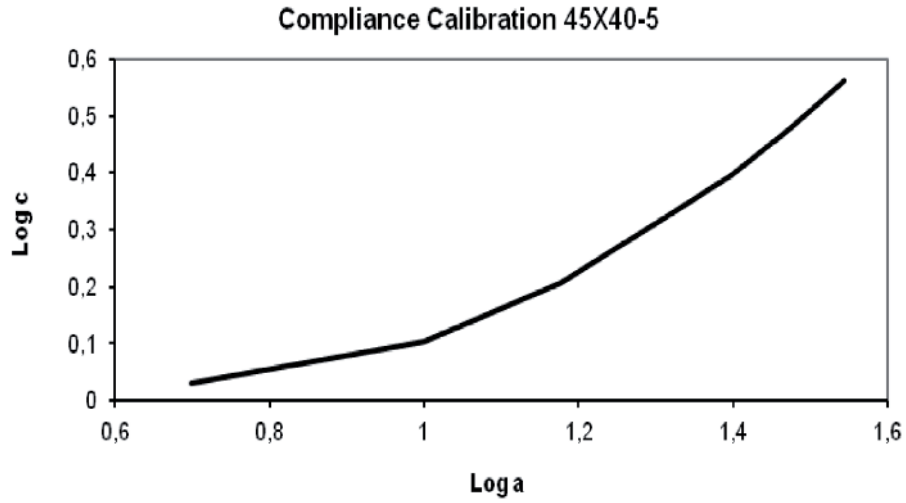

Figure 14.
Curve for slope of log c vs. log a, 'n' for sample 5 woven $[\pm 45^\circ]_{16}$ with 40 mm width.

The fracture toughness can be obtained as the function of crack length. In the case of a plane strain condition, the relationship between G_{IC} and K_{IC} is given as follows:

$$G_{IC} = \frac{K_{IC}^2}{E}\left(1-\nu^2\right) \tag{5}$$

where E is the modulus of elasticity, ν is the Poisson's ratio.

The average G_{IC} values are compared and drawn with error bars for 4 types of samples with different width and are given in **Figure 15a** and **b**. As it is seen from the figure, the influence of width on average G_{IC} for [0°/90°] fiber orientation specimens, and [±45°] fiber orientation specimens for different width is small or in other words, as the increasing width of specimen there is a little decrease in average SERR value.

For materials with high interlaminar fracture toughness, it may be necessary to increase the number of plies, that is, increase the laminate thickness or decrease the

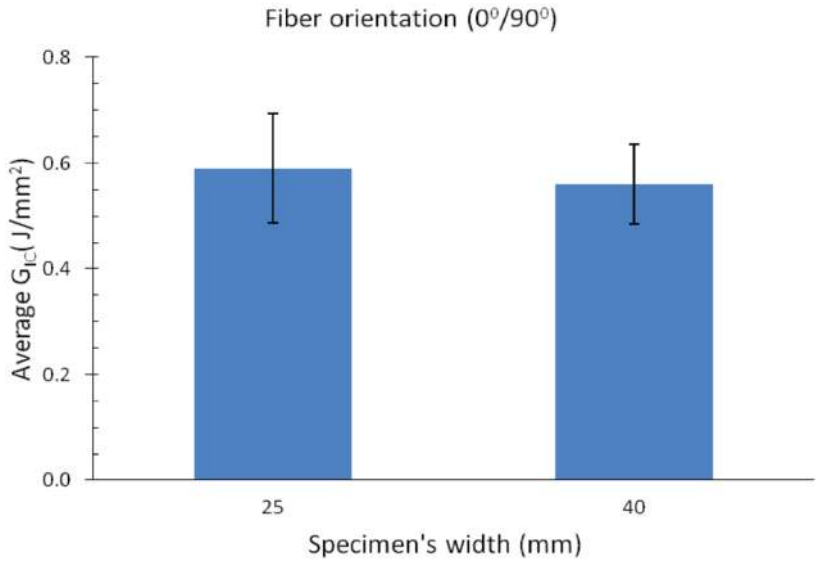

Figure 15.
Influence of width on average G_{IC} for a) [0°/90°] fiber orientation specimens, b) [±45°] fiber orientation specimens. Error bars are ± 1 standard deviations.

delamination length. Thus, for most studies the results indicate a trend of increasing propagation G_{IC} values with increasing DCB thickness [27].

4. Numerical analysis

In the numerical study, the entire specimen was modeled using solid layered 46 element in ANSYS 12.1. Specimens with 25 mm width have 25000 mesh elements

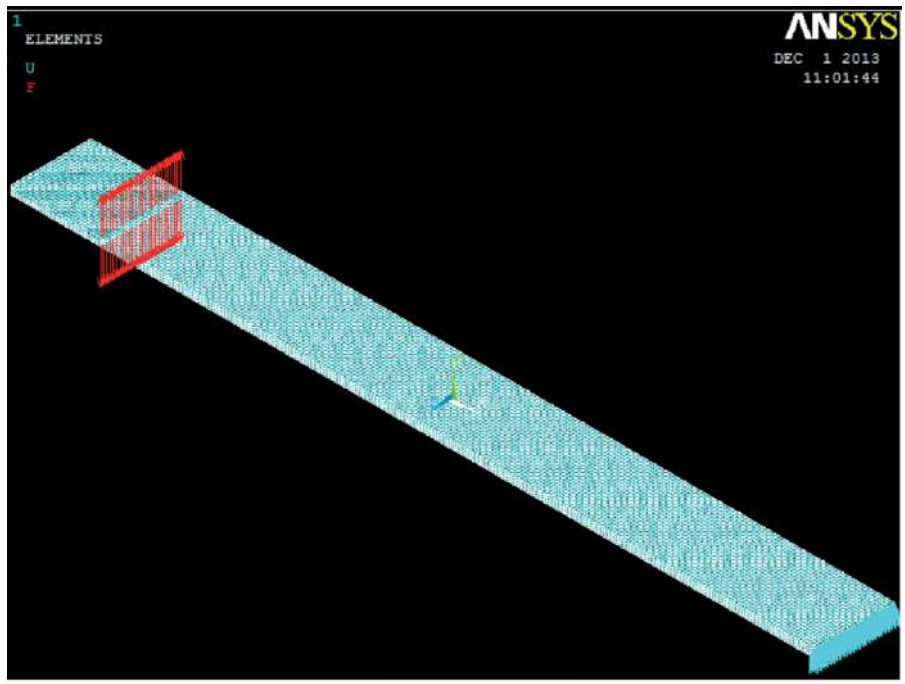

Figure 16.
Detailed view of FEM model of DCB test specimen used under loading.

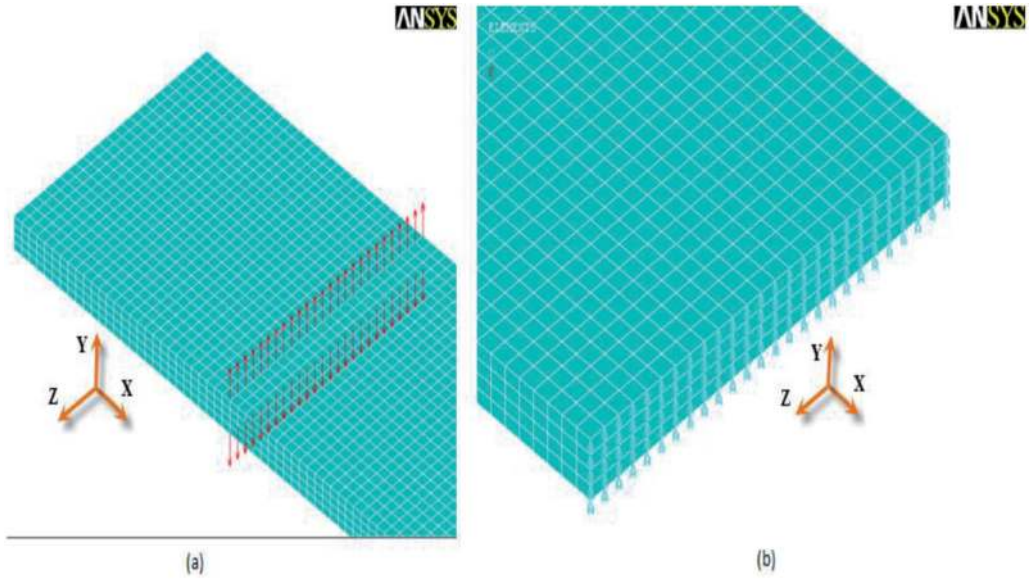

Figure 17.
Forces and boundary conditions of FEM: a) nodal forces, b) boundary conditions.

and specimens with 40 mm width have 40000 mesh elements. A linear elastic finite-element analysis was performed under a plane strain condition. The loads corresponding to the crack initiation in the DCB tests were used to the finite element solution (see in **Figure 16**).

As a part of study, the variation of versus different width length has been investigated. The load was applied as a nodal force at the upper and bottom layer of the composite as shown in **Figure 17(a)** and all nodes along the right side of the composite were restrained in y direction as shown in **Figure 17(b)**. The mechanical properties, which were obtained experimentally, of woven-fabric-reinforced glass/epoxy composite materials are given in **Table 1** and were used during the analysis. The numerical analysis results of the fracture toughness that was obtained by FEM are given in **Table 3**. It is seen that, the obtained numerical values are good comparability with the corresponding experimental results for all experiment groups. As a result of numerical analyses, it can be seen that the fracture toughness increases slightly relative to the amount of decreasing width as mentioned in ASTM D 5528–01 standards, it means that the change of width of DCB specimen is not a great effective parameter for interlaminar fracture toughness values.

The results of experiment tests and numerical analysis showed good agreement demonstrating the effectiveness of the proposed experiment and numerical methods.

***DCB* specimen type**	**Average G_{IC} (J/mm^2)**	**K_{IC} ($MPa\sqrt{m}$) experimental results**	**K_{IC} ($MPa\sqrt{m}$) ANSYS results**
0° × 25 (woven)	0.586	4.076	4.170
0° × 40 (woven)	0.563	3.984	4.110
45° × 25 (45° woven)	0.544	2.600	2.530
45° × 40 (45° woven)	0.530	2.560	2.480

Table 3.
Interlaminar fracture toughness of the woven and woven 45 with different width.

5. Results and discussion

Delamination in composites can occur due to tensile stress Mode I. In the present study, AG-50kNG Shimadzu universal testing machine (see in **Figure 5**) has been used to record the load-deflection curves for calculating fracture toughness for DCB specimen and **Figure 6** shows the initial and the progress of fracture in the machine. Specimens have been designed by referring ASTM standards, DIN EN ISO 75-1, 75–3. The woven $[0°/90°]_{16}$ and woven $[\pm45°]_{16}$ specimens made up of woven-fabric-reinforced glass/epoxy composite materials were studied and the mechanical properties and interlaminar fracture toughness K_{IC} value were obtained experimentally by using DCB and numerically by using FEM. Four types of tests were performed. Each of them includes five tests corresponding to combinations of different stacking sequence of woven and width. For the DCB specimens, the delamination was generated during manufacturing by placing teflon between the mid-layer therefore an initial delamination or crack was formed. In this experiment, the output data have been recorded and graphs have been plotted as required.

The mean values for every individual test groups can be shown in **Figures 11–14**. The SERR, G_{IC} can be derived from the recorded load–displacement data by using compliance calibration method and Eq. (2) to determine Mode I interlaminar fracture toughness K_{IC} given in **Table 3**. The average G_{IC} value of (0°/90°) fiber orientation specimens, for different width with error bars are ±1 standard deviations and the influence of width on average G_{IC} for (±45°) fiber orientation are shown with error bars are ±1 standard deviations in **Figure 15a** and **b**, respectively. It has been obtained that woven $[0°/90°]_{16}$ specimens have higher fracture toughness values than, woven $[\pm45°]_{16}$ specimens to show the effect of different lay-up,.

Figures 7–10 show a typical load–displacement curves for woven $[0°/90°]_{16}$ and woven $[\pm45°]_{16}$ specimens, respectively. According to ASTM 5528–1 the loading process consists of two steps. In step1, the loading was continued with crosshead speed 2 mm/min up to the displacement of about 28 mm and until the first crack propagation Δa 2–3 mm occurs. Then the crosshead was returned to zero point with 25 mm/min constant displacement speed to form a natural pre-crack. In the step 2, second loading was continued with crosshead speed 2 mm/min up to the displacement of about 80 mm, and after then the crosshead was returned to zero point with 25 mm/min constant displacement speed. It is seen that, some degree of non-linearity and small permanent deformations were visible in the unloading curves of specimens. The non-linearity can be partly attributed to the specimens undergoing relatively large displacements towards the end of the tests.

As it is seen from the **Table 3**, the fracture toughness values decrease 2.20% in percentage for the woven $[0°/90°]_{16}$ specimens 25 mm and 40 mm in width, while the specimen width increases. Similarly, for woven $[\pm45°]_{16}$, the fracture toughness values decrease 1.27% in percentage, while the specimen width increases. In other words, the energy release rate increases slightly with decreasing width length for both type of woven specimens. Also it is seen that, the obtained fracture toughness value of woven $[0°/90°]_{16}$ specimen with 25 mm width is greater 3.93% than woven $[\pm45°]_{16}$ specimen. Similarly, it has been found that the fracture toughness value of woven $[0°/90°]_{16}$ specimen 40 mm in width is greater 2.96% than woven $[\pm45°]_{16}$ specimens 40 mm in width.

The obtained average maximum load and the critical SERR, G_{IC} achieved from Eqs. (1) and (2) for plane strain case, have been given in **Table 2**. In the finite element analysis, the stress intensity factor K_{IC} was obtained for DCB specimens numerically. The comparison of experimental and numerical results of K_{IC} values are given in **Table 3**. Finite element analysis was conducted to validate the closed

form solution. Results show a good agreement between analytical solutions, numerical simulation shown as in **Table 3**. As it is seen from the table, the differences between numerical and analytical solutions are approximately 2.31–2.69% percentage for 25 mm width specimen and 3.13–3.16% percentage for 40 mm width specimen. It can be said that, when the width range increases the differences between the numerical and analytical solutions may change small amount because of meshing type at delamination through thickness.

6. Conclusion

The problems of interlaminar performance are discussed along with the technique used to measure them and the fracture mechanics principles applied to improve them. The DCB test is a well established test used to measure interlaminar fracture toughness in reinforced composite materials. In this study, interlaminar fracture toughness values are determined by DCB test method Mode I for woven $[0°/90°]_{16}$ and woven $[\pm 45°]_{16}$ glass/epoxy composite materials. For investigation of woven angles and specimens width's effect on fracture toughness have been compared. It has been obtained that woven $[0°/90°]_{16}$ specimens have higher fracture toughness values than, woven $[\pm 45°]_{16}$ specimens. Some decreases has been eventuated in fracture toughness values by an increase on width. Also, the energy release rate increases with decreasing width length. Therefore, width effect for DCB specimens on fracture toughness value can be neglected. It is also seen that here its no special effect of width on SERR for DCB test specimens. The agreement between the calculated results and the experimental data shows that the finite element analysis method is reliable.

The thickness of material is an important parameter between the state of plane stress and plane strain, and the fracture toughness value can be obtained. For materials with high interlaminar fracture toughness, it may be necessary to increase the number of plies, that is, increase the laminate thickness or decrease the delamination length.

Author details

Evren Meltem Toygar[1*] and Ahmet Gulakman[2]

1 Department of Industrial Engineering, Dokuz Eylül University, Izmir, Turkey

2 Graduate School of Nature and Applied Sciences, Dokuz Eylül University, Izmir, Turkey

*Address all correspondence to: evren.toygar@deu.edu.tr

References

[1] Aliyu AA, Daniel IM. Effects of strain rate on delamination fracture toughness of graphite epoxy. American Society for Testing and Materials. 1985. p. 336-348

[2] Davidson BD, Kruger R, Konig. Effect of stacking sequence on energy release rate distributions in multidirectional DCB and ENF specimens. Engineering Fracture Mechanics. 1996;55(4):557-569.

[3] Sun CT, Zheng S. Delamination characteristics of double cantilever beam and end-notched flexure composite specimens. Composites Science and Technology. 1996;56:451-459.

[4] Toygar M.E., Toparli M. and Uyulgan B., An investigation of fracture toughness of carbon/epoxy composites. Journal of Reinforced Plastics and Composites. 2006;25(18): 1887-1895.

[5] De Morais AB, De Moura MF, Marques AT, De Castro PT. Mode I interlaminer fracture of carbon/epoxy cross–ply composites. Composites Science and Technology. 2002;62:679-686.

[6] Hyer MW. Stress Analysis of Fiber Reinforced Composite Materials. Boston, Massachusetts: McGraw-Hill, 1998.

[7] Broek D. Elemantary Engineering Fracture Mechanics. Boston, Massachusetts: Kluwer Academeic Publishers, 1996.

[8] Jones RM. Mechanics of Composite Materials. Leviitown, PA: Taylor and Francis, 1999.

[9] O'Brien TK. Fracture mechanics of composite delamination. Composites: ASM International. 2001;21:241-245.

[10] O'Brien TK. Characterization of Delamination Onset and Growth in a Composite Laminate, Composite Materials: Testing and Design. Philadelphia: ASTM STP 775, American Society for Testing and Materials. 1982. p. 140-167.

[11] Tay TE. Characterization and analysis of delamination fracture in composites – An overview of developments from 1990 to 2001. Applied Mechanics Reviews. 2003;56:1-32.

[12] ASTM Standard D 5528-01. Standard test method for mod 1 interlaminar fracture toughness of unidirectional fiber-reinforced polymer matrix composites. Philadelphia: Annual Book of ASTM Standards. 1984;3:1.

[13] BS ISO 15024. Fiber-reinforced plastic composites—Determination of mode-I interlaminar fracture toughness, G_{IC}, for unidirectionally reinforced materials. British: Standard, United Kingdom.

[14] M.N. Durakbasa, P.H. Osanna, P. Demircioglu, The factors affecting surface roughness measurements of the machined flat and spherical surface structures – The geometry and the precision of the surface, Measurement, 2011;44(10), 1986-1999.

[15] DIN EN ISO 75-1, Kunststoffe. Bestimmung der Wärmeformbeständigkeitstemperatur. Teil 1: Allgemeines Prüfverfahren (ISO 751:2004);Deutsche Fassung EN ISO 751:2004, September 2004.

[16] DIN EN ISO 75-3, Kunststoffe. Bestimmung der Wärmeformbeständigkeitstemperatur. Teil 3: Hochbeständige härtbare Schichtstoffe und langfaserverstärkte Kunststoffe (ISO 753:2004); Deutsche

Fassung EN ISO 753:2004, September 2004.

[17] J.H. Chen et al. Effect of fibre content on the interlaminar fracture toughness of unidirectional glass-fibre/ polyamide composite. Composites: Part A 1999;30: 747-755.

[18] Martin RH, Murri GB. Characterization of mode I and mode II delamination growth and thresholds in AS4/PEEK composites. Composite materials: Testing and design. Philadelphia: ASTM STP 1059. American Society for Testing and Materials. 1990;9:251-270.

[19] O'Brien TK. Towards a Damage Tolerance Philosophy for Composite Materials and Structures. Composite Materials: Testing and Design. Philadelphia: ASTM STP 1059, American Society for Testing and Materials. 1990. p.7-33.

[20] Russell AJ, Street KN. A Constant G Test for Measuring Mode I Interlaminar Fatigue Crack Growth Rates. In: Proceedings of Composite Materials: Testing and Design (Eighth Conference). Philadelphia: ASTM STP 972, American Society for Testing and Materials. 1988. p.259-277.

[21] Whitney JM, Browning CE, Hoogsteden W. A double cantilever beam test for characterizing mode I delamination of composite materials. Reinforced Plastics and Composites 1982; 1: 297-313.

[22] ASTM Standard E6-81. Standard Definitions of Terms Relating to Methods of Mechanical Testing. Annual Book of ASTM Standards. Philadelphia: ASTM, 1981. p.187-196.

[23] Zhang Z. Research and Development Facilities in Advanced Polymer and Composites (APC) Research Group. Portsmouth, UK, 2010. http://www.port.ac.uk/research/composites/filetodownload,106518,en.pdf (Accessed 06 April 2013).

[24] Reder C., Loidl D., Puchegger S., Gitschthaler D., Peterlik H., Kromp K., Khatibi G., Betzwar-Kotas A., Zimprich P., Weiss B., Non-contacting strain measurements of ceramic and carbon single fibres by using the laser-speckle method, Composites: Part A 2003; 34:1029-1033.

[25] Anderson TL. Fracture Mechanic: Fundamental and Applications. CRC Press, 2nd edition, 1995.

[26] M.S. Sham Prasad, C.S. Venkatesha, T. Jayaraju. Experimental methods of determining fracture toughness of fiber reinforced polymer composites under various loading conditions. Journal of Minerals & Materials Characterization & Engineering, 2011;10(13), 1263-1275.

[27] Hojo M., Aoki T. Thickness Effect of Double Cantilever Beam Specimen on Interlaminar Fracture Toughness of AS4/PEEK and T800/Epoxy Laminates in, Composite Materials, Fatique and Fracture, Fourth Volume, ASTM STP 1156, W. W. Stinchcomb and N. E. Ashbaugh (Eds), ASTM, Philadelphia, 2007;281-298.